1 Introduction

Particle accelerators were originally developed for research in nuclear and high-energy physics for probing the structure of matter. Over the years advances in technology have allowed higher and higher particle energies to be attained thus providing an ever more microscopic probe for understanding elementary particles and their interactions. To achieve maximum benefit from such accelerators, measuring and controlling the parameters of the accelerated particles is essential. This is the subject of this book.

In these applications, an ensemble of charged particles (a 'beam') is accelerated to high energy, and is then either sent onto a fixed target, or collided with another particle beam, usually of opposite charge and moving in the opposite direction. In comparison with the fixed-target experiments, the center-of-mass energy is much higher when colliding two counter-propagating beams. This has motivated the construction of various 'storage-ring' colliders, where particle beams circulate in a ring and collide with each other at one or more dedicated interaction points repeatedly on successive turns. A large number of particles, or a high beam current, is desired in almost all applications. The colliders often require a small spot size at the interaction point to maximize the number of interesting reactions or 'events'.

The charged particles being accelerated are typically electrons, positrons, protons, or antiprotons, but, depending on the application, they can also be ions in different states of charge, or even unstable isotopes. Often the beams consist of several longitudinally separated packages of particles, so-called 'bunches', with empty regions in between. These bunches are formed under the influence of a longitudinal focusing force, usually provided by the high-voltage rf field, which also serves for acceleration.

If the trajectory of a high-energy electron or positron is bent by a magnetic field, it emits energy in the form of synchrotron radiation. The energy loss per turn due to synchrotron radiation increases with the fourth power of the beam energy and decreases only with the inverse of the bending radius. This limits the energy attainable in a ring collider. The maximum energy ever obtained in a circular electron-positron collider – more than 104 GeV per beam – was achieved in the Large Electron Positron Collider (LEP) at the European laboratory CERN in Geneva, Switzerland, with a ring circumference of almost 27 km.

The most promising option for accomplishing electron-positron collisions at even higher energy are linear colliders, where the two beams are rapidly accelerated in two linear accelerators ('linacs') and collide only once. In order to obtain a reasonable number of interesting events, the spot sizes at the collision point must be much smaller than those obtained in all previous colliders. Design values for the root-mean-square (rms) vertical spot size at the collision point are in the range 1–6 nm, for center-of-mass energies between 500 GeV and 3 TeV. The one and only high energy linear collider to date is the Stanford Linear Collider (SLC), which was operated from 1988–1998 at Stanford University in California. The SLC collided electrons and positron beams with an energy of about 47 GeV each, and the vertical rms beam size at the collision point varied between 500 nm and 2 μm. In order to be able to achieve the small spot size, the beam must have a high density; e.g., a small emittance.

A positive feature of the synchrotron radiation is that at lower energy it leads to a shrinkage of the beam volume in a storage ring via radiation damping. The beam volume is usually characterized in terms of three emittances, which are proportional to the area in the phase space occupied by the beam for each degree of motion. The radiation damping acts with a typical exponential time constant of a few ms. This damping property is exploited in the linear-collider concept by first producing a high-quality dense beam in a damping ring, at a few GeV energy, prior to its acceleration in a linear accelerator (which consists essentially of a long series of accelerating rf cavities with intermediate transverse focusing by quadrupole magnets of alternating polarity) and subsequent collision.

Synchrotron radiation itself is also used directly for numerous applications in biology, material science, X-ray lithography, e.g., for microchip fabrication, and medicine, to mention a few. Many synchrotron radiation centers have been established all over the world. In these facilities, the photon beam quality depends on the properties of the electron or positron beam stored in the ring, thus placing high demands on the beam quality and trajectory control, similar to those required by the colliders.

Recent developments have demonstrated the possibility to produce substantially (6–7 orders of magnitude) brighter light at even shorter wavelength. These are based on the coherent amplification of photons spontaneously emitted as an extremely dense beam traverses a series of alternating bending magnets with short period (an 'undulator') in a single pass. This concept of a free-electron laser (FEL) based on self-amplified spontaneous emission (SASE) presently draws much attention around the world. While in a conventional light source, the light power increases in proportion to the number of particles, in a SASE FEL it increases in proportion to its square.

There are many other types of accelerators and their uses, not all of which can be covered in detail in this book. Noteworthy are perhaps the ion or pion

accelerators which are used for cancer therapy, and of which there are several in operation, e.g., in Canada and Japan.

We also note that, unlike the collider operation, in the preparation of high-intensity proton beams for a fixed target, the emittance is often intentionally diluted, so that the beam fills the entire available aperture. This 'painting' stabilizes the beam and reduces the effect of the beam space-charge forces. Also in this case performance may further be improved by optics corrections and by a more precise knowledge of the beam properties.

In Tables 1.1, 1.2, and 1.3 we list a selection of typical parameters for a few ring colliders, linear colliders, and light sources, respectively.

Table 1.1. Parameters of Storage Ring Colliders

Variable	Symbol	Tristan	PEP-II	KEKB	HERA	LEP	LHC
Species		e^+e^-	e^+e^-	e^+e^-	$pe^\pm$	e^+e^-	pp
Beam energy [GeV]	E_b	30	9, 3.1	8, 3.5	920, 27.5	104	7000
No. of bunches	n_b	2	1658	5000	174	4	2800
Bunch population [10^{10}]	N_b	20	2.7, 5.9	1.4, 3.3	10, 4	40 40	11 11
Rms IP beam size [µm]	$\sigma_{x,y}^*$	300, 8	157, 4.7	90, 1.9	112, 30	250, 3	16
Normalized rms emittance [µm]	$\gamma\epsilon_{x,y}$	6000, 90	400, 15 (e^+)	125, 2.5 (e^+)	5, 1000	8000, 40	3.75
Circumference [km]	C	3.02	2.20	3.02	6.34	26.66	26.66

The reaction rate in a collider, R, is given by the product of the cross section of the reaction σ and the luminosity L:

$$R = \sigma L. \tag{1.1}$$

Considering two beams with Gaussian transverse profiles of rms size σ_x (in the horizontal direction) and σ_y (in the vertical direction), with $N_{b,1}$ and $N_{b,2}$ the number of particles per bunch per beam respectively, the luminosity for head-on collisions is expressed by

$$L = \frac{f_{\mathrm{coll}} N_{b,1} N_{b,2}}{4\pi\sigma_x\sigma_y}, \tag{1.2}$$

with f_{coll} the average bunch collision frequency. In a storage ring, the number of particles per bunch N_b is related to the total stored current I by

Table 1.2. Parameters of (Planned) Linear Colliders

Variable	Symbol	FFTB	SLC	NLC	TESLA	CLIC
Beam energy [GeV]	E_b	47	47	250	250	1500
No. of bunches / train	n_b	1	1	190	2820	154
Rep. rate [Hz]	n_b	10	120	120	5	100
Bunch population [10^{10}]	N_b	0.5	4	0.75		0.4
Rms IP beam size [nm]	$\sigma^*_{x,y}$	60 (y)	1400, 500	245, 2.7	553, 5	43, 1
Normalized rms emittance [µm]	$\gamma\epsilon_{x,y}$	2 (y)	50, 8	3.6, 0.04	10, 0.03	0.58, 0.02
Luminosity [10^{34} cm^{-2}s^{-1}]	L	—	2×10^{-4}	2	3.4	10

Table 1.3. Parameters of Light Sources and SASE FELs

Variable	Symbol	ALS	ESRF	SPring-8	TTF FEL	TESLA FEL
Beam energy [GeV]	E_b	1.5	6	8	1	15–50
No. of bunches	n_b	300	662	1760	800	11500/ pulse
Bunch population [10^{10}]	N_b	0.5	0.5	0.2	0.6	0.6
Rms beam size [µm]	$\sigma_{x,y}$	200, 31	400, 20	150, 20	50	27
Norm. transv. emittance [µm]	$\gamma\epsilon_{x,y}$	10, 0.7	47, 0.35	94, 0.04	2	1.6
Bunch length [mm]	σ_z	4.0	4.0	4.0	0.05	0.025

$$I = n_t n_b N_b e \frac{f_{\mathrm{rf}}}{h} , \qquad (1.3)$$

where n_t is the number of trains, n_b is the number of bunches per train, e is the electric charge, f_{rf} is the accelerating frequency, and h is the harmonic number. The rms beam sizes $\sigma_{x,y}$ are related to the beam volume, or to the emittance, and to a focusing parameter $\beta_{x,y}$, via $\sigma_{x,y} = \sqrt{\epsilon_{x,y}\beta_{x,y}}$. Hence, for a linear collider smaller emittances $\epsilon_{x,y}$ translate into higher luminosity[1]. In (1.2), we have omitted a number of correction factors, which are sometimes

---

[1] for storage ring colliders this is not necessarily true since $N_b/\epsilon_{x,y}$ may be limited by the beam-beam interaction

important. For example, if the beta functions at the collision point are comparable or smaller than the bunch length, the luminosity is lower than that predicted by (1.2). This is referred to as the 'hourglass effect'. In addition, at high current the focusing force of the opposing beam may significantly change the single-particle optics. As a result, the beta functions at the interaction point either increase or decrease ('dynamic beta function'), and the luminosity changes accordingly.

The parameter describing the photon-beam quality of a synchrotron-radiation light source is the spectral brightness B, which refers to the photon flux in the six-dimensional phase space. Again considering a Gaussian beam, and assuming that the beam sizes are above the photon diffraction limit ($\epsilon_{x,y} > \lambda_\gamma/4\pi$, where λ_γ is the photon wavelength), the average spectral brightness at frequency ω is

$$B(\omega) = \frac{C_\psi EIS(\omega/\omega_c)}{4\pi^2\epsilon_x\epsilon_y}\,,\tag{1.4}$$

where E is the beam energy, I the beam current, $C_\psi = 4\alpha/(9em_ec^2) \approx 3.967\times10^{19}$ photons / (sec rad A GeV), where α is the fine structure constant,

$$S(\omega/\omega_c) = \frac{9\sqrt{3}}{8\pi}\frac{\omega}{\omega_c}\int_{\omega/\omega_c}^\infty K_{5/3}(\bar{x})\,\mathrm{d}\bar{x}\,,\tag{1.5}$$

and $\omega_c \equiv (3/2)c\gamma^3/\rho$ the critical photon frequency (where ρ is the bending radius, and γ the electron beam energy divided by the rest energy m_ec^2). The important point is that the average spectral brightness depends strongly on the beam emittance and on the beam current.

In this book we will describe commonly used strategies for the control of charged particle beams and the manipulation of their properties. These are strategies aimed towards improving the accelerator performance and meeting the ever more demanding requirements. Emphasis is placed on relativistic beams in storage rings and linear accelerators. Only one chapter is devoted to problems associated with low energy beams. We assume that the reader is familiar with fundamental accelerator optics as described, for example, in [1, 2, 3, 4]. In the remainder of this introduction we nonetheless review some fundamentals of accelerator optics thereby also introducing the notations to be used in this text. In the following chapters, we discuss basic and advanced methods for measuring and controlling fundamental beam properties, such as transverse and longitudinal lattice diagnostics and matching procedures, orbit correction and steering, beam-based alignment, and linac emittance preservation. Also to be presented are techniques for the manipulation of particle beam properties, including emittance measurement and control, bunch length and energy compression, bunch rotation, changes to the damping partition number, and beam collimation issues. Finally, we discuss a few special topics, such as injection and extraction methods, beam cooling, spin transport, and polarization.

The different techniques are illustrated by examples from various existing or past accelerators, for example, the large electron-positron collider LEP [5] at CERN, the SLAC PEP-II B factory [6], the linac of the KEK B factory [7], the Stanford Linear Collider (SLC) [8, 9], TRISTAN at KEK [10], the synchrotron light sources SPEAR at SLAC [11] and the ALS at Berkeley [12], the CERN Low Energy Antiproton Ring (LEAR) [13], the Accelerator Test Facility (ATF) at KEK [14], the electron-proton collider HERA at DESY [15], the final-focus test beam at SLAC [16], the CERN $p\bar{p}$ collider SPS [17], the ASSET experiment at SLAC [18], the TESLA Test Facility at DESY [19], the FNAL recycler ring [20], RHIC [21], and the ISR at CERN [22]. At various places, we also refer to planned or proposed future accelerators, such as the Large Hadron Collider [23], the Next Linear Collider [24], the TESLA Linear Collider [25], and the Muon Collider [26].

## 1.1 Review of Transverse Linear Optics

We can distinguish two types of accelerator systems: rings and transport lines both with and without acceleration. In a storage ring the optical functions, such as the dispersion D or the beta function β, are well defined by the periodic boundary conditions. For a transport line, on the other hand, there is no such boundary condition, and here it is convention to determine the initial values of the optical functions from the initial beam size and the correlations contained in the initial beam distribution (see (1.17–1.19)).

Often a 3-dimensional coordinate system (x, s, y) is employed to describe the particle motion, where the local tangent to s points in the direction of the beam line, x is directed in the radial outward direction, and y in the vertical upward direction. These coordinates are illustrated in Fig. 1.1. In a beam line without any bending magnets, or if there is bending in more than one plane, some ambiguity exists in the definition of the x and y. While s gives the location around the ring, the particle coordinates x and y measure the transverse distance from an ideal reference particle, e.g., a particle passing through the center of perfectly aligned quadrupole magnets. Further, it is customary to introduce a second longitudinal coordinate $z = s - v_0 t$ where v_0 denotes the velocity of the ideal particle and t the time. The coordinate z thus measures the longitudinal distance to the ideal reference, which may be taken to be the center of the bunch. For example, if $z > 0$ the particle is moving ahead of the bunch center and arrives earlier in time than the bunch center at an arbitrary reference position.

In a linear approximation, the transverse motion of a single particle in an accelerator can be described as the sum of three components [4, 27]

$$u(s) = u_{\text{c.o.}}(s) + u_\beta(s) + D_u(s)\delta,\qquad(1.6)$$

where $u(s) = x(s)$ or $y(s)$ is the horizontal or vertical coordinate at the (azimuthal) location s. Here $u_{\text{c.o.}}$ denotes the closed equilibrium orbit (or,
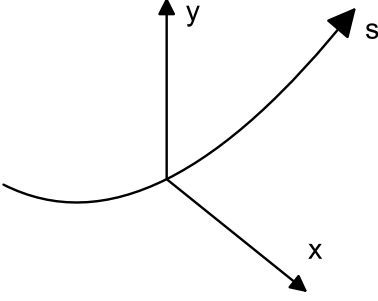
Fig. 1.1. Schematic of the reference trajectory and the transverse coordinate system

in a transport line, some reference trajectory), u_β the orbit variation due to betatron motion (transverse oscillations), and $D_u\delta$ the orbit change resulting from an energy offset; D_u is the dispersion function, and $\delta = \Delta p/p$ is the relative deviation from the design momentum given by the difference of the particle momentum from the design momentum both divided by the design momentum.

The beam is transversely focused by quadrupole magnets usually of alternating polarity. The linear equation of motion for the horizontal motion is

$$\frac{\mathrm{d}^2 x}{\mathrm{d}s^2} = -k(s)x\,, \tag{1.7}$$

where x is the offset from the quadrupole center. The focusing coefficient $k(s)$ is given in units of m^{-2} and is nonzero only in a quadrupole field, in which it is given by

$$k = \frac{B_T}{(B\rho)a}\,, \tag{1.8}$$

where B_T denotes the quadrupole pole-tip field, a the pole-tip radius, and

$$B\rho\ [\mathrm{T-m}] \approx 3.356\ p\ [\mathrm{GeV/c}] \tag{1.9}$$

is the magnetic rigidity in units of Tesla-meters. Often, especially in large acclerators, one can employ a 'thin-lens' or 'kick' approximation, and express the effect of the quadrupole simply by a change in the trajectory slope $x' \equiv dx/ds$ according to

$$\Delta x' = -Kx\,, \tag{1.10}$$

where

$$K \equiv kl_{\mathrm{quad}} \tag{1.11}$$

is the integrated strength of the quadrupole in units of m^{-1} and l_{quad} is the quadrupole length. Here and in the following, we use the prime to signify a derivative with respect to the longitudinal position s.

Note that the strength of other magnets can be normalized to the beam momentum in a similar way as for quadrupoles. As an example, we consider a

sextupole magnet. This is a nonlinear element which is often installed in storage rings at a location with nonzero dispersion and is used for correcting the variation of the quadrupole focusing strength with the particle momentum, i.e., the chromaticity. The local sextupole field in units of m^{-3} is expressed as $m = 2B_T/(a^2(B\rho))$, where B_T now denotes the sextupole pole-tip field, and the integrated sextupole strength becomes $M = ml_{\text{sext}}$. In a kick approximation, the effect of the sextupole on the horizontal trajectory slope is $\Delta x' = Mx^2/2$.

In the remainder of this section, however, we ignore the effect of nonlinear elements and restrict the discussion to particle trajectories with small amplitudes, which evolve according to the linear optics. Then, for constant beam energy, the horizontal or vertical betatron motion, i.e., the solution to (1.7), can be parametrized by a pseudo-harmonic oscillation of the form [4]

$$u_{\beta,x,y}(s) = \sqrt{2I_{x,y}\beta_{x,y}(s)} \, \cos(\phi_{x,y}(s) + \phi_0), \tag{1.12}$$

where $\beta_{x,y}(s)$ is called the beta function, $\phi_{x,y}(s)$ the betatron phase ('angle variable'), and $I_{x,y}$ is an 'action variable'. Action variables are known from classical mechanics. There the Hamiltonian of a harmonic oscillator is expressed by $H(I,\phi,\theta) = QI$, where θ is a time-like variable and Q is a constant equal to the number of oscillations per revolution (in accelerator physics this is called the 'tune'). In the absence of nonlinear perturbations and using a proper choice of coordinates, the betatron motion in an accelerator can be described by exactly the same Hamiltonian as the harmonic oscillator.

In addition to the beta function β, two closely related functions are often introduced to characterize the betatron motion. These are

$$\alpha(s) = -\frac{1}{2}\beta'(s) \qquad \text{and} \qquad \gamma(s) = \frac{1+\alpha^2(s)}{\beta(s)}, \tag{1.13}$$

where as before the prime indicates a derivative with respect to the longitudinal position s, and we have dropped the subindex 'x,y'. Together β, α, and γ are referred to as the Twiss parameters. Henceforth, we will use x instead of u, but, here and in the following, the same equations apply in the horizontal and in the vertical plane. The main difference is that quadrupoles which are focusing in one plane are defocusing in the other.

The functions $\phi_{x,y}(s)$ and $\beta_{x,y}(s)$ in (1.12) vary with the azimuthal location s, while the action $I_{x,y}$ and initial phase ϕ_0 are constants of motion. The beam is matched to the lattice if the betatron phases are distributed randomly. In this case, the value of $I_{x,y}$ averaged over all particles of the beam is equal to the rms beam emittance. For example, in the horizontal plane, we then have

$$\epsilon_x^{rms} \equiv \sigma_x^2/\beta_x = \langle I_{x,y}\rangle \tag{1.14}$$

and

$$I_x = \frac{x_\beta^2 + (\beta_x x_\beta' + \alpha_x x)^2}{\beta_x}. \tag{1.15}$$

The 'betatron oscillation' described by (1.12) refers to a particle at a fixed design energy. Later, we will discuss how the motion is modified if the energy is not constant, introducing the two concepts of dispersion and chromaticity.

If the beam is accelerated, as in a linac, the beam energy is not constant and the right-hand side of (1.12) must be multiplied by $\sqrt{\gamma(0)/\gamma(s)}$, since the increase in longitudinal momentum p_s reduces the transverse beam size by effectively introducing a damping force $d^2x/ds^2 \approx -p_x/p_s^2 \, dp_s/ds$. Inside an accelerating structure with energy gradient E', the formula for α becomes

$$\alpha(s) = -\frac{\beta'(s)}{2} + \frac{\beta E'(s)}{2E(s)}, \tag{1.16}$$

$E(s)$ is the beam energy at location s.

The three optical functions $\beta(s)$, $\alpha(s)$ and $\gamma(s)$ are proportional to the three second moments of the beam distribution, with the rms beam emittance as the constant of proportionality:

$$\langle x^2 \rangle_s = \beta(s) \, \epsilon, \tag{1.17}$$

$$\langle xx' \rangle_s = -\alpha(s) \, \epsilon, \tag{1.18}$$

$$\langle x'^2 \rangle_s = \gamma(s) \, \epsilon, \tag{1.19}$$

where $\langle \ldots \rangle_s$ denotes an average over the beam distribution at the location s. Thus, the actual values of β, α and γ can be deduced from the measured beam distribution. It is a challenge to the accelerator physicist to make them coincide with their design values.

In a storage ring, the optical functions α, β and γ are periodic: $\beta(s) = \beta(s+C)$, $\alpha(s) = \alpha(s+C)$, and $\gamma(s) = \gamma(s+C)$, where C is the ring circumference. For a transport line, or linac, no such periodic boundary condition exists; and the values of the optical functions depend on the incoming beam distribution, e.g., via (1.17), (1.18), and (1.19).

Another description, alternative to the 'Twiss parameters' (α, β and γ) represents the motion of a single particle in terms of a transport matrix [28, 29]. Here, a trajectory is denoted by a point in the phase space (x, x') which is transformed from the initial location i to a new (final) location f through a linear transformation

$$\begin{pmatrix} x \\ x' \end{pmatrix}_f = \begin{pmatrix} R_{11} & R_{12} \\ R_{21} & R_{22} \end{pmatrix}_{fi} \begin{pmatrix} x \\ x' \end{pmatrix}_i. \tag{1.20}$$

This can also be generalized to a (6×6) transport matrix for motion with coupling between the horizontal, vertical and longitudinal planes. In the 6-dimensional case, the vector (x, x') is replaced by $(x, x', y, y', z, \delta)$, where δ is the relative energy error and z is the longitudinal distance to a co-moving reference particle, are the coordinates in the longitudinal phase space.

Let us review a few examples. In lowest-order approximation, for a drift space of length l, the 2-dimensional transport matrix is

$$\mathbf{R}_{\mathrm{drift}} = \begin{pmatrix} 1 & l \\ 0 & 1 \end{pmatrix} . \tag{1.21}$$

The matrix for a focusing quadrupole of gradient $k = (\partial B/\partial x)/(B\rho)$ and of length l_q is

$$\mathbf{R}_{\mathrm{quad}} = \begin{pmatrix} \cos\phi & \sin\phi/\sqrt{|k|} \\ -\sqrt{|k|}\sin\phi & \cos\phi \end{pmatrix} , \tag{1.22}$$

where $\phi = l_q\sqrt{|k|}$. If we take the limit of vanishing quadrupole length $l_{\mathrm{quad}} \to 0$ while holding the integrated gradient $K = |k| l_q$ constant, we arrive at the matrix for an idealized 'thin-lens' quadrupole

$$\mathbf{R}_{\mathrm{thin-lens}} = \begin{pmatrix} 1 & 0 \\ -K & 1 \end{pmatrix} . \tag{1.23}$$

Thus, the focal length of the thin quadrupole is given by $1/K$. The R matrix for a sequence of quadrupoles and drift spaces is simply the product of the R matrices for the individual elements.

It is important to note that the description in terms of optical functions and the R matrix formalism are equivalent and complementary. We can transform the optical functions from one location to another using the elements of the R matrix:

$$\begin{pmatrix} \beta \\ \alpha \\ \gamma \end{pmatrix}_f = \begin{pmatrix} R_{11}^2 & -2R_{11}R_{12} & R_{12}^2 \\ -R_{11}R_{21} & 1+2R_{12}R_{21} & -R_{12}R_{22} \\ R_{21}^2 & -2R_{21}R_{22} & R_{22}^2 \end{pmatrix}_{fi} \begin{pmatrix} \beta \\ \alpha \\ \gamma \end{pmatrix}_i . \tag{1.24}$$

Alternatively, we can express the elements of the R matrix from i to f in terms of the optical functions at the initial and final locations,

$$\mathbf{R}_{fi} = \begin{pmatrix} \sqrt{\frac{\beta_f}{\beta_i}}(\cos\phi_{fi} + \alpha_i\,\sin\phi_{fi}) & \sqrt{\beta_f\beta_i}\,\sin\phi_{fi} \\ -\frac{1+\alpha_f\alpha_i}{\sqrt{\beta_f\beta_i}}\,\sin\phi_{fi} + \frac{\alpha_i-\alpha_f}{\sqrt{\beta_f\beta_i}}\,\cos\phi_{fi} & \sqrt{\frac{\beta_i}{\beta_f}}\,(\cos\phi_{fi} - \alpha_f\,\sin\phi_{fi}) \end{pmatrix} , \tag{1.25}$$

where $\phi_{fi} = (\phi_f - \phi_i)$ is the betatron phase advance between the two locations.

In a storage ring, one can compute the 1-turn matrix by demanding that the final location f is equal to the initial one i, after a full revolution. The matrix (1.25), or one-turn-map (OTM), then simplifies to

$$\mathbf{R}_{\mathrm{otm}} = \begin{pmatrix} \cos\mu + \alpha\,\sin\mu & \beta\,\sin\mu \\ -\gamma\sin\mu & \cos\mu - \alpha\,\sin\mu \end{pmatrix} , \tag{1.26}$$

where μ denotes the 1-turn phase advance. The betatron tune Q or ν, is defined as the number of betatron oscillations per turn. It is related to the 1-turn phase advance μ by $Q \equiv \nu = \mu/(2\pi)$.

We note explicitly that the tranport matrices for a single particle and for the beam centroid are identical at low beam currents and without nonlinearities.

1.2 Beam Matrix

The beam distribution can be characterized by its first and second moments.
The first moments give the centroid motion. The second moments are com-
bined in a 'beam matrix'. For example, the beam matrix Σ_{beam} for the hori-
zontal plane is defined as

$$
\begin{aligned}
\Sigma_{\text{beam}}^x &= \epsilon_x \begin{pmatrix} \beta & -\alpha \\ -\alpha & \gamma \end{pmatrix} \\
&= \begin{pmatrix} \langle x^2 \rangle - \langle x \rangle^2 & \langle xx' \rangle - \langle x \rangle \langle x' \rangle \\ \langle x'x \rangle - \langle x' \rangle \langle x \rangle & \langle x'^2 \rangle - \langle x' \rangle^2 \end{pmatrix} .
\end{aligned}
\tag{1.27}
$$

Here α, β, and γ are the ellipse (e.g., Twiss) parameters (compare (1.17–
1.19), and Fig. 1.2), ϵ is the beam emittance, and the bracketed terms are
various moments of the beam distribution, i.e., $\langle x \rangle$ is the first moment, or
mean, of the distribution in position, $\langle x' \rangle$ is the first moment, or mean, of
the distribution in angle, and $\langle x^2 \rangle$, $\langle x'^2 \rangle$ are the second moments of the beam
distribution. Specifically, for a beam intensity distribution $f(x)$,

$$
\langle x \rangle = \frac{\int\limits_0^\infty x f(x)\, \mathrm{d}x}{\int\limits_0^\infty f(x)\, \mathrm{d}x} ,
\tag{1.28}
$$

and

$$
\langle x^2 \rangle = \frac{\int\limits_0^\infty x^2 f(x)\, \mathrm{d}x}{\int\limits_0^\infty f(x)\, \mathrm{d}x} .
\tag{1.29}
$$

The root-mean-square (rms) of the distribution σ_x is (usually) the physical
quantity of interest:

$$
\sigma_x = \sqrt{\langle x^2 \rangle - \langle x \rangle^2} .
\tag{1.30}
$$

If the mean of the distribution is neglected (i.e., either disregarding the static
position offset of the core of the beam, or defining the coordinates with respect
to this offset), (1.27) reduces to

$$
\Sigma_{\text{beam}}^x = \begin{pmatrix} \langle x^2 \rangle & \langle xx' \rangle \\ \langle xx' \rangle & \langle x'^2 \rangle \end{pmatrix}
\tag{1.31}
$$

and the rms of the distribution is simply $\sigma_x = \langle x^2 \rangle^{\frac{1}{2}}$.
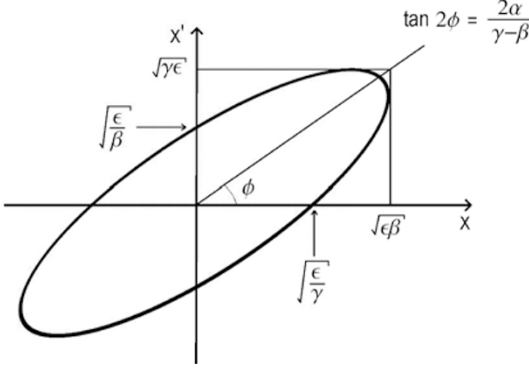
Fig. 1.2. Ellipse parameters for the beam matrix [28, 29]

The transformation between an initial beam matrix $\Sigma_{\mathrm{beam},0}$ to the beam matrix Σ_{beam} at a desired observation point is

$$\Sigma_{\mathrm{beam}} = R\Sigma_{\mathrm{beam},0}R^t \,, \tag{1.32}$$

where R is the transfer matrix and R^t is the transpose of R. Here, depending on how many degrees of freedom are considered, Σ_{beam} and R can be 2×2, 4×4 or 6×6 matrices. For an uncoupled system, the 4×4 matrix $\Sigma_{\mathrm{beam}}^{xy}$, characterizing the transverse beam distribution in the horizontal and vertical phase space, is of block-diagonal form:

$$\Sigma_{\mathrm{beam}}^{xy} = \begin{pmatrix} \Sigma_{11} & \Sigma_{12} & 0 & 0 \\ \Sigma_{21} & \Sigma_{22} & 0 & 0 \\ 0 & 0 & \Sigma_{33} & \Sigma_{34} \\ 0 & 0 & \Sigma_{43} & \Sigma_{44} \end{pmatrix} \,, \tag{1.33}$$

and

$$R = \begin{pmatrix} R_{11} & R_{12} & 0 & 0 \\ R_{21} & R_{22} & 0 & 0 \\ 0 & 0 & R_{33} & R_{34} \\ 0 & 0 & R_{43} & R_{44} \end{pmatrix} \,. \tag{1.34}$$

Note that the $\Sigma_{\mathrm{beam}}^{xy}$-matrix is symmetric with $\Sigma_{12}^{xy} = \Sigma_{21}^{xy}$ (cf. (1.27)) but that, in general, $R_{12} \neq R_{21}$.

1.3 Review of Longitudinal Dynamics

If the energy of the beam, or of a particle in the beam, differs from the design energy its trajectory may deviate from the trajectory of an ideal particle which has the desired energy. In first order, this deviation is linear in the momentum deviation $\delta = \Delta p/p$ (p here is the nominal momentum). For

a transport line we can write the horizontal displacement resulting from the energy error as

$$\Delta x(s) = R_{16}\delta \,, \tag{1.35}$$

where R_{16} is the (1,6) transport matrix element from the location where the energy error δ was induced to the location s. In a (planar) storage ring, the orbit deviation due to an energy offset is given by the periodic dispersion function $D_x(s)$ as

$$\Delta x(s) = D_x(s)\delta \,. \tag{1.36}$$

Also, in a transport line, the R_{16} matrix element of (1.35) is often called dispersion, but it should be kept in mind that this term is not uniquely defined as the measured values depend on the location where an energy change is introduced (and may be different from the real energy-position correlation within the bunch). As a result, the correction of dispersion in a transport line or a linac can become conceptually quite complicated.

If the beam (or particle) energy is varied, the radius of curvature and, thus, the path length in the bending magnet changes. The first order path length change is characterized by the momentum compaction factor α_c:

$$\alpha_c = \frac{\Delta C/C}{\delta} = \frac{1}{C}\oint \frac{D(s)}{\rho(s)}\ \mathrm{d}s \,. \tag{1.37}$$

If $\gamma > 1/\sqrt{\alpha_c}$, a ring is said to operate 'above transition'; this is the case for most electron and high-energy proton rings. For a transport line, one may replace α_c in (1.37) by the R_{56} matrix element, and D_x by R_{16}, and consider

$$R_{56}(s) = \int_{s_0}^{s} \frac{R_{16}(s')}{\rho(s')}\ \mathrm{d}s' \,. \tag{1.38}$$

Just as the beam, or an individual particle in the beam, executes betatron oscillations, it also performs oscillations in the longitudinal phase space, e.g., in a storage ring with nonzero rf voltage. The frequency of the synchrotron motion is usually much lower than the betatron-oscillation frequencies (one synchrotron period typically corresponds to 100s of turns). It can be expressed in terms of a synchrotron tune Q_s (which is the synchrotron frequency f_s in units of the revolution frequency f_{rev}):

$$Q_s = \frac{f_s}{f_{\mathrm{rev}}} = \sqrt{\frac{(\alpha_c - \gamma^{-2})he\hat{V}\sin\phi_s}{2\pi\beta cp_0}} \,, \tag{1.39}$$

where α_c again is the momentum compaction factor, $\hat{V}$ the amplitude of the rf voltage (assumed as simply cosine-like: $V_{\mathrm{rf}} = \hat{V}\cos(\omega_{\mathrm{rf}}t + \psi)$), h the rf harmonic number ($f_{\mathrm{rf}} = hf_{\mathrm{rev}}$), e the particle charge, p_0 the equilibrium momentum, c the speed of light, and ϕ_s the synchronous phase angle measured with respect to the crest of the rf. The latter is determined by the equality $e\hat{V}\cos\phi_s = U_0$, where U_0 is the average energy loss per turn, and by the condition for phase stability is $0 < \psi_s < \pi/2$ above transition. The transition energy corresponds to $Q_s = 0$.

1.4 Transverse and Longitudinal Equations of Motion

The smooth approximation to the beam motion considers only the average focusing force and ignores the discrete locations of rf cavities or quadrupole magnets. In the longitudinal plane, we assume further that the oscillations are small compared with the amplitude of the focusing rf wave so that only the linear part of the sinusoidal rf force is sampled by the beam. With these approximations both longitudinal and transverse oscillations are then described by the equation of a harmonic oscillator.

In the transverse plane

$$x'' + (\omega_\beta/c)^2 x \quad = 0 \,, \tag{1.40}$$

$$p_x{}'' + (\omega_\beta/c)^2 p_x = 0 \,, \tag{1.41}$$

with $p_x \equiv (\alpha x + \beta x')$, where ω_β/c^2 is the appropriate average of $k(s)$ in (1.7) and $\omega_\beta = 2\pi Q$. In the longitudinal plane

$$\phi'' + \omega_s^2 \phi = 0 \,, \tag{1.42}$$

$$\delta'' + \omega_s^2 \delta \ = 0 \,, \tag{1.43}$$

with $\phi' = (\alpha_c - (1/\gamma)^2)\omega_{\mathrm{rf}}\delta$ and $\omega_s = 2\pi f_s$.

The second moments of the beam distribution have an immediate physical significance. For example, $\sigma_x = \langle x^2 \rangle^{\frac{1}{2}}$ is the horizontal rms beam size, $\sigma_{x'} = \langle x'^2 \rangle^{\frac{1}{2}}$ the horizontal rms beam divergence, $\sigma_y = \langle y^2 \rangle^{\frac{1}{2}}$ the vertical rms beam size, $\sigma_{y'} = \langle y'^2 \rangle^{\frac{1}{2}}$ the vertical rms beam divergence, $\sigma_z = \langle z^2 \rangle^{\frac{1}{2}}$ the rms bunch length (or, in terms of rf phase, $\sigma_\phi = \omega_{\mathrm{rf}}\sigma_z/c$), and $\sigma_\delta = \langle \delta^2 \rangle^{\frac{1}{2}}$ the rms momentum spread.

For completeness we list the beam matrix Σ_{beam} for a transverse (e.g., horizontal) plane,

$$\Sigma_{\mathrm{beam}}^x = \begin{pmatrix} \langle x^2 \rangle & \langle xx' \rangle \\ \langle xx' \rangle & \langle x'^2 \rangle \end{pmatrix} \,, \tag{1.44}$$

and its analogue for the longitudinal one,

$$\Sigma_{\mathrm{beam}}^z = \begin{pmatrix} \langle \phi^2 \rangle & \langle \phi\delta \rangle \\ \langle \delta\phi \rangle & \langle \delta^2 \rangle \end{pmatrix} \,. \tag{1.45}$$

The transverse and longitudinal emittances are obtained from

$$\epsilon_x = \sqrt{\det \Sigma_{\mathrm{beam}}^x} = \sqrt{\langle x^2 \rangle \langle x'^2 \rangle - \langle xx' \rangle^2} \,, \tag{1.46}$$

$$\epsilon_y = \sqrt{\det \Sigma_{\mathrm{beam}}^y} = \sqrt{\langle y^2 \rangle \langle y'^2 \rangle - \langle yy' \rangle^2} \,, \tag{1.47}$$

and

$$\epsilon_z = \sqrt{\det \Sigma_{\mathrm{beam}}^z} = \sqrt{\langle \phi^2 \rangle \langle \delta^2 \rangle - \langle \phi\delta \rangle^2} \,, \tag{1.48}$$

where det denotes the determinant of the corresponding matrix. It is common to consider the normalized emittances $\epsilon_{x,y,N} \equiv \gamma\beta\epsilon_{x,y}$ and $\gamma\beta\epsilon_z$ which are constant under acceleration (here β and $\gamma = 1/\sqrt{1 - \beta^2}$ are the relativistic factors).

Exercises

1.1 Beam Emittance in Terms of Action Angle Variables

Individual particles within a bunch (index i) perform betatron oscillations, which can be described in terms of action-angle variables by $x_i(s) = \sqrt{2I_x \beta_x(s)} \cos \phi_x(s)$. Consider a beam whose distribution function depends only on the action variable; i.e., $\rho(I_x, \phi_x) = \rho(I_x)/(2\pi)$. Define the horizontal emittance as $\epsilon_x = \langle x^2(s) \rangle / \beta_x(s)$. Show that $\epsilon_x = \langle I_x \rangle$, where the square brackets denote an average over the beam distribution at location s.

1.2 Projected Beam Emittances

a) Consider now a 2-dimensional particle distribution which is Gaussian and uncorrelated in the 4 variables x_0, x_0', y_0 and y_0' with emittances ϵ_{x0} and ϵ_{y0}. Suppose the beam passes a skew quadrupole of strength K_s with beta functions at the quadrupole equal to β_x and β_y. Afterwards the coordinates of the new distribution are x, x', y and y'. They are correlated as

$$x' = x_0' + K_s y_0 \,, \qquad (1.49)$$
$$y' = y_0' + K_s x_0 \,, \qquad (1.50)$$
$$x = x_0 \,, \qquad (1.51)$$
$$y = y_0 \,. \qquad (1.52)$$

Calculate the beam matrix in terms of the Twiss parameters and the initial uncoupled emittances.

b) The projected horizontal and vertical emittances are given by the square root of the determinant of the 2×2 submatrices. Calculate the projected emittances and express them in terms of the initial uncoupled emittances, and the skew quadrupole strength K_s.